



Immobilization-Enhanced Eradication of Bacterial Biofilms and in situ Antimicrobial Coating of Implant Material Surface – an in vitro Study

This article was published in the following Dove Press journal:
International Journal of Nanomedicine

Hien A Tran ¹⁻⁴
Phong A Tran ¹⁻⁴

¹School of Chemistry, Physics and Mechanical Engineering, Faculty of Science and Engineering, Queensland University of Technology (QUT), Brisbane, Queensland, Australia;

²Interface Science and Materials Engineering (ISME) Group, QUT, Brisbane, Queensland, Australia; ³Centre in Regenerative Medicine, QUT, Brisbane, Queensland, Australia; ⁴Institute of Health and Biomedical Innovation, Kelvin Grove, Queensland, Australia

Purpose: The aim of this study was to investigate a new method of in situ biofilm treatment for infected prostheses that remove bacterial biofilm and prevent reinfection through the use of an immobilizing agent in combination with the actions of biofilm-lysing enzymes and bactericidal antimicrobials.

Methods: We investigated the combination of self-immobilization chemistry of dopamine with a biofilm-lysing enzyme, α -amylase (Am), and an antimicrobial agent, silver nitrate (Ag), to treat model *Staphylococcus aureus* (*S. aureus*) biofilms formed on titanium. The efficacy of biofilm removal and bacterial treatment was analyzed by crystal violet, colony-forming unit assays, confocal laser scanning microscopy, and scanning electron microscopy (SEM). To confirm the in situ coating of the titanium surface with antimicrobial Ag as a strategy to prevent bacterial recolonization, SEM in secondary electron mode (SE), backscatter electron mode, (BSE) and energy-dispersive spectroscopy (EDX) were used. The antimicrobial activity of the coated surface was evaluated by optical density measurement and colony-forming unit assays.

Results: Polydopamine (PDA)-assisted treatment showed approximately a 2 log reduction in recoverable CFU and a 15% increase in biofilm removal efficacy compared to treatments that had only Am or Ag. More importantly, PDA-assisted treatment was found to immobilize Ag on the surface after the treatment, rendering them resistant to bacterial recolonization.

Conclusion: Our in vitro findings suggested that this PDA-assisted treatment and the surface immobilization-enhanced treatment concept could be promising in the development of advanced treatment for implant retention surgery for an infected prosthesis.

Keywords: bacterial biofilm, in situ treatment, implants, antimicrobial, coatings

Introduction

There is a significant research interest in developing novel therapies for periprosthetic joint infection to improve surgery outcomes. Surgical options for this condition such as in infected total knee arthroplasty can be broadly divided into i) single- or two-stage implant exchange surgery and ii) implant retention surgery.¹⁻⁴ The former is highly invasive and results in significantly reduced mobility.⁵ In addition, if the prosthesis was used with bone cement, its removal can cause significant damage to the host bone and could lead to further complications. Hence, for a certain population of patients such as in acute infection cases, it is sometimes recommended to perform implant retention surgery which is much less invasive.^{6,7}

Commonly recommended for acute infections (up to 3 months after initial arthroplasty with ongoing symptoms of joint infection under 3 weeks), implant

Correspondence: Phong A Tran
Tel +61 7 3138 6452
Email phong.tran@qut.edu.au

retention surgery involves extensive debridement to remove bacteria and bacterial biofilms on the implant and surrounding tissue while the implant is retained.^{6–10} The patients are then often treated with local or systemic antibiotics for an extended period (up to 8 weeks). Usually known as debridement, antibiotics and implant retention (DAIR) surgery, the procedure's success rate is often reported between 60% and 80% and is recognized as strongly dependent on removal efficacy of the strongly adhered bacterial biofilm from implant's surface and deactivation of associated bacteria.^{11–13} Hence, the success rates have been found to vary significantly depending on multiple factors such as the duration of infection, infectious organism, patient conditions and can be as low as 9% in certain cases.^{6,7,9,10,14} The treatment is even much less effective and generally not recommended for more chronic infections.^{6,14–17}

Different methods have been developed to enhance the efficacy of in situ biofilm removal and prevent reinfection with limited success due to multiple factors, for example the treatment needs to take place in situ; in other words, the methods to destroy biofilm and deliver antimicrobials need to be appropriate for intraoperative use.^{18,19} Another important factor is that current approaches often overlook the importance of making the implant resistant to reinfection.^{20–26} Since bacterial recolonization of the retained implant can lead to recurrent infection, it is important that the implant surface becomes resistant to such an event through, for example, antimicrobial coatings. This preventive measure is particularly important for implant retention surgeries as it has been suggested that in certain patient populations, a lifelong antibiotic suppression regime might be necessary to prevent infection recurrence.¹⁰

In this context, we aimed to develop a new method to eradicate the established biofilms and associated bacteria on implants in situ and at the same time, coating the implant surface with antimicrobial to prevent reinfection. In our design, to eradicate established bacterial biofilms and associated bacteria, we chose to use a biofilm-destroying enzyme α -amylase (Am)^{27–32} and antimicrobial silver (Ag).^{33–35} This enzyme has been extensively investigated for treating established biofilm. Similarly, antimicrobial Ag and Ag nanoparticles have also been extensively studied and demonstrated broad antimicrobial activities.^{36,37}

Combination of enzymatic treatment and antimicrobial has been reported before; yet in this current study, we developed a new concept of immobilization-enhanced treatment and exploited the versatile polymerization and surface self-immobilization chemistry of dopamine.^{38–41}

Dopamine has been widely used as an oxidation-induced polymerization and self-immobilizing agent for coating a nanometer-thick polydopamine (PDA) layer at slightly alkaline pH (approximately 8.5) on a range of substrate chemistries including metals, ceramics, and polymers.⁴² Importantly, the PDA layers were shown to be able to sequester metal ions from a solution and reduce them into immobilized submicron-/nano-particles.^{39,43–45} In this concept, the surface self-immobilization of PDA is exploited to not only enhance the biofilm removal and bacterial killing efficacy of Am and Ag but also concurrently immobilize Ag on the surface of implants in situ to make it antimicrobial.

In this study, we demonstrated the proof of our concept by treating *S. aureus* biofilm formed on titanium substrates as a model for in situ treatment of periprosthetic joint infection.

Materials and Methods

Materials

Titanium (Ti) plates were purchased from A&E metals (New South Wales, Australia) (Grade 2, 0.7 mm thick). Ti plates were cut into 1 cm in diameter discs, cleaned with acetone and ethanol, and sterilized by autoclaving at 121°C for 20 mins.

α -Amylase (Am) powder was purchased from MP Biomedical (New South Wales, Australia). The Am powder was dissolved in sterile PBS to get 1% (w/v) in final concentration. The solution was then sterilized by filtering through a 0.2- μ m filter membrane and stored at 4°C.

Silver nitrate (Ag) powder was purchased from Sigma-Aldrich Company (New South Wales, Australia). The 100 μ g/mL of the Ag solution was prepared by dissolving silver nitrate powder in sterile MilliQ water.

Dopamine hydrochloride (DA), sodium carbonate (Na₂CO₃), and sodium bicarbonate (NaHCO₃) were also purchased from Sigma-Aldrich Company (New South Wales, Australia). DA stock solution was prepared by dissolving DA powder in MilliQ water to get 100 g/L in final concentration and stored at 4°C.

Syto9 was purchased from Thermo Fisher Scientific (New South Wales, Australia). The staining working solution was prepared by dissolving Syto9 stock solution in 0.85% NaCl to get a 5 μ M solution.

Growth Condition and Treatment

S. aureus (ATCC 25293) was grown in the Lysogeny broth (LB) Agar plate overnight. Several overnight cultured colonies

were then added into the Mueller Hinton (MH) broth. A spectrophotometer (xMark, Biorad) was used to adjust the absorbance of the bacterial suspension at 600 nm to 0.5 McFarland standard (approximately 1.5×10^8 CFU/mL).⁴⁶ Forty microliters of this suspension was dropped onto the surface of the Ti discs which were placed in a 48-well plate. Next, the samples were incubated for 48 hrs before a new MH broth was added and incubated for another 48 hrs.

After incubation, the samples were rinsed in sterile MilliQ water to remove planktonic bacteria prior to being divided into 4 groups receiving different treatments as follows.

Group 1 (G1: PDA-Assisted Treatment)

Step 1: Incubating in dopamine solution: the samples were first immersed in the polymerization solution of dopamine which was freshly prepared by diluting 10 μ L of DA stock solution in 1 mL of 0.1 M $\text{Na}_2\text{CO}_3/\text{NaHCO}_3$ buffer (pH 8.5) at room temperature for 30 mins following gentle rinsing 2 times in sterile MilliQ water.

Step 2: Incubating in enzyme solution: The samples were then immersed in the Am enzyme solution (1% w/v) at 37°C for 30 mins. The samples were then rinsed 2 times in sterile MilliQ water.

Step 3: Incubating in dopamine solution for the second time: The samples were then immersed again in the polymerization solution of dopamine which was freshly prepared by diluting 10 μ L of DA stock solution in 1 mL of 0.1 M $\text{Na}_2\text{CO}_3/\text{NaHCO}_3$ buffer (pH 8.5) at room temperature for 30 mins following gentle rinsing 2 times in sterile MilliQ water.

Step 4: Incubating in Ag solution: The samples were then immersed in the Ag solution 100 μ g/mL at room temperature for 30 mins. The samples were then rinsed 2 times in sterile MilliQ water.

In group 2 (G2: enzyme and antimicrobial only treatment), the samples were immersed in Am solution (as in step 2) and then Ag solution (as in step 4). In group 3 (G3: enzyme only treatment), the samples were immersed in the enzyme solution (as in step 2). Untreated samples are in group 4 (G4-control) and used as the control.

Crystal Violet (CV) Assay

After the treatment, all the samples were immersed in 0.1% (CV) (Sigma-Aldrich, New South Wales, Australia) solution for 15 mins before being dipped twice in MilliQ water to remove the unbound dye. After that, the samples were left dry overnight at room temperature. Samples were then immersed in 30% acetic acid for 15 mins to solubilize the bound CV. One hundred microliters of the extracted solution

were then transferred into a 96-well plate and its absorbance was measured at 550 nm using a spectrophotometer (xMark, Biorad). The experiments were performed in triplicates ($n=3$) and repeated 5 times.

Bacteria Staining and Imaging

To visualize the bacteria, the samples after the treatment were rinsed in 0.85% NaCl prior to being immersed in a Syto9 staining solution 5 μ M in the dark for 15 mins and rinsed again with 0.85% NaCl to remove the unbound dye. The samples were imaged using confocal laser scanning microscopy (CLSM) (Nikon A1R, Nikon) with 488 nm laser excitation and 500–530nm bandpass emission. The images were processed using Nikon A1R software. The experiments were performed in duplicates ($n=2$) and repeated 2 times.

Colony-Forming Unit (CFU) Assay

In a separate set of samples, the samples after the treatment were rinsed in sterile MilliQ water and placed in 15-mL falcon tubes containing 3 mL of sterile PBS. They were then vortexed and sonicated for 90 s. The supernatant was collected, serially diluted in sterile PBS, and plated on LB agar plates and incubated at 37°C overnight and the number of colonies was recorded. The results were then converted into log CFU for the analysis. The experiments were performed in duplicates ($n=2$) and repeated 5 times.

Scanning Electron Microscopy (SEM) Imaging

In a separate set of samples, the samples after the treatment were fixed with 4% paraformaldehyde at 4°C for 30 mins. Then, samples were dehydrated with increasing ethanol concentrations (70%, 80%, 90%, 95%, and 100%) for 10 mins at each dilution. After that, the samples were incubated in hexamethyldisilazane (HMDS) at room temperature for 30 mins before being re-incubated in fresh HMDS and let dry in a fume hood for 24 hrs. All the samples were gold coated (Leica EM SCD005, Leica) before imaging with a scanning electron microscope (Sigma FESEM, Zeiss).

Some samples after the SEM fixation procedure as described earlier were carbon coated (Cressington 208 Carbon, Cressington) and used for SEM in secondary electron (SE), backscatter electron (BSE) modes, and an energy-dispersive X-ray spectroscopy (EDX). The SE images were then assigned a green color and BSE red before merging to create pseudo-color composite images

using ImageJ software. The experiments were performed in duplicates ($n=2$) and repeated 2 times.

Antimicrobial Activity of the Surface After the Treatment

The samples after the treatment were transferred to 48-well plate prior to being added with 1 mL of sterile MH broth to each well. The samples were incubated at 37°C for 3 days. At each day, 100 μL of the solution in each well was transferred to a 96-well plate to measure the absorbance at 600 nm using the spectrophotometer (xMark, Biorad) and 100 μL of fresh MH broth was re-added to each well. The experiments were performed in duplicates ($n=2$) and repeated 2 times.

In a separate set of samples, the samples in group 1 (PDA-assisted treatment) were sterilized by immersing in 80% ethanol for 30 mins followed by exposure to ultraviolet light for 20 mins. The samples were left to dry completely and then rinsed with sterile PBS before being put in a 48-well plate. Then, the samples were added with 200 μL of MH broth containing *S. aureus* which was diluted 100 times from McFarland 0.5 to obtain approximately 1.5×10^6 CFU/mL. The same volume of bacteria was also added to fresh sterile Ti discs as a control. The samples were incubated for 24 hrs at 37°C, and the number of recoverable CFU was determined using CFU assay as described earlier. The experiments were performed in duplicates ($n=2$) and repeated 3 times.

Statistical Analysis

All the graphs were constructed using GraphPad Prism 8, while the statistical data were analyzed using SPSS software.

The statistical data were presented in the form of mean \pm standard error of the mean. The significant difference was analyzed using Kruskal–Wallis one-way of analysis of variance (ANOVA) and Wilcoxon 2-sample rank-sum. * $p < 0.05$; ** $p < 0.01$

Results

PDA-Assisted Treatment Enhanced Biofilm Removal

We first investigated the effects of combination treatment on biofilm removal. To do this, we applied the treatment on bacterial biofilm formed on Ti substrates and used CV assays to measure the remained biofilm. α -Amylase (Am)-alone treatment removed $65 \pm 8.7\%$ of the biofilm, while Am and silver nitrate (Ag) treatment removed $72 \pm 10\%$, and PDA-assisted Am-Ag treatment removed $83 \pm 6.1\%$ of the biofilm (Figure 1A). No significant difference was found between Am-alone and Am-Ag treatment. PDA-assisted Am-Ag treatment was significantly more effective than Am-alone ($p < 0.05$) and Am-Ag treatment.

We also investigated the treatment efficacy using confocal laser scanning microscopy (CLSM). The biofilm on untreated samples (Group 4) appeared as a thick and dense layer, indicating a mature bacterial biofilm (thickness of approximately $28.1 \pm 5.8 \mu\text{m}$, Figure 1B–G4). Am-alone treatment disrupted approximately 60% biofilms and resulted in a thickness decrease to $22.2 \pm 3.5 \mu\text{m}$ (Figure 1B–G3). The Am-Ag treatment significantly reduced the biofilm and thickness ($20.8 \pm 3.4 \mu\text{m}$), indicating the contribution from Ag (Figure 1B–G2). PDA-assisted Am-Ag treatment (Group 1) sharply reduced biofilm and its thickness (maximum

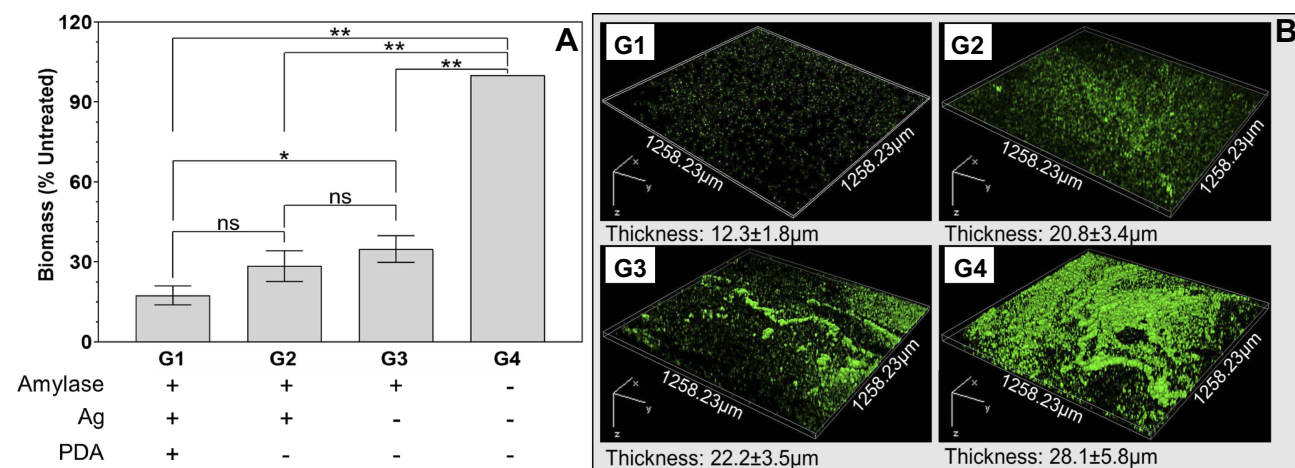


Figure 1 PDA-assisted treatment-enhanced biofilm removal. (A) Biofilm biomass measured by crystal violet assay (data = mean \pm standard error of the mean, $n=5$, * $p < 0.05$, ** $p < 0.001$). (B) Representative confocal laser scanning microscopy images of samples after the treatments (bacteria appeared green) and associated biofilm thickness.

measured thickness of $12.3 \pm 1.8 \mu\text{m}$). In fact, the majority of bacteria found on the surface of samples in Group 1 appeared as nonaggregated individual bacteria (Figure 1B–G1). These results showed that PDA-assisted treatment significantly enhanced biofilm removal efficacy.

PDA-Assisted Treatment Enhanced Bacteria Killing

Next, we evaluated the effect of the treatments on bacteria viability by CFU assays and SEM imaging. The log CFU results showed that all the treated groups had reduced log CFU compared to the untreated control. Untreated samples had 6.9 ± 1.1 log CFU and Am-only treatment had 6.1 ± 0.7 log CFU (no significant reduction compared to the untreated group) (Figure 2A). Meanwhile, Am-Ag treatment had 4.2 ± 0.6 log CFU and PDA-assisted treatment had 2.2 ± 1.9 log CFU. The results thus demonstrated a significant reduction of log CFU on samples receiving Am-Ag treatment (2.7 log reduction, $p < 0.05$) and on samples receiving PDA-assisted treatment (nearly 5 log reduction, $p < 0.001$) compared to the untreated group. The bacteria in samples receiving PDA-assisted treatment also exhibited abnormal morphology similar to a damaged membrane, likely caused by antimicrobial actions of Ag nanoparticles (Figure 2B–G1).^{47–49}

PDA-Assisted Treatment Rendered the Surface Antimicrobial

We further evaluated the effectiveness of PDA-assisted treatment on bacteria deactivation by incubating the

substrates in bacteria-free culture broth and measured the cloudiness of the broth during incubation as an indicator of bacterial growth (Figure 3A – regrowth test). After 1 day, the optical density of the broth for sample in Group 1, PDA-assisted treatment, was about 0.007 indicating no growth of bacteria (transparent broth), while other groups had an optical density of approximately 0.2 clearly indicating bacterial growth (cloudy broth) (Figure 3B and D). However, after 2 and 3 days, regrowth of bacteria was observed in all groups (Figure 3B), indicating that the effect diminished after 2 days.

We next tested if the treated surface could inhibit bacteria recolonization (Figure 3A – antibacterial test). In a separate set of samples after the biofilm treatment, we applied *S. aureus* suspension to the treated substrates, incubated for 1 day, and determined log CFU. The substrates receiving PDA-assisted treatment had significantly lower log CFU (log CFU of 7.9 ± 0.4 , $p < 0.05$) than the bare substrates (log CFU of 9.1 ± 0.5) (Figure 3C), suggesting that the PDA-assisted treatment provided the substrate with antimicrobial activity.

The Antimicrobial Activity of the Treated Surface Was Attributable to the Surface Immobilization of Ag

First, the PDA coating layer was visible as a typical brown staining of the samples (Figure 4A4).⁴²

To confirm our hypothesis that PDA assisted the immobilization of Ag, we used SEM coupled with EDX to study the sample surface. The EDX results showed that the immobilized

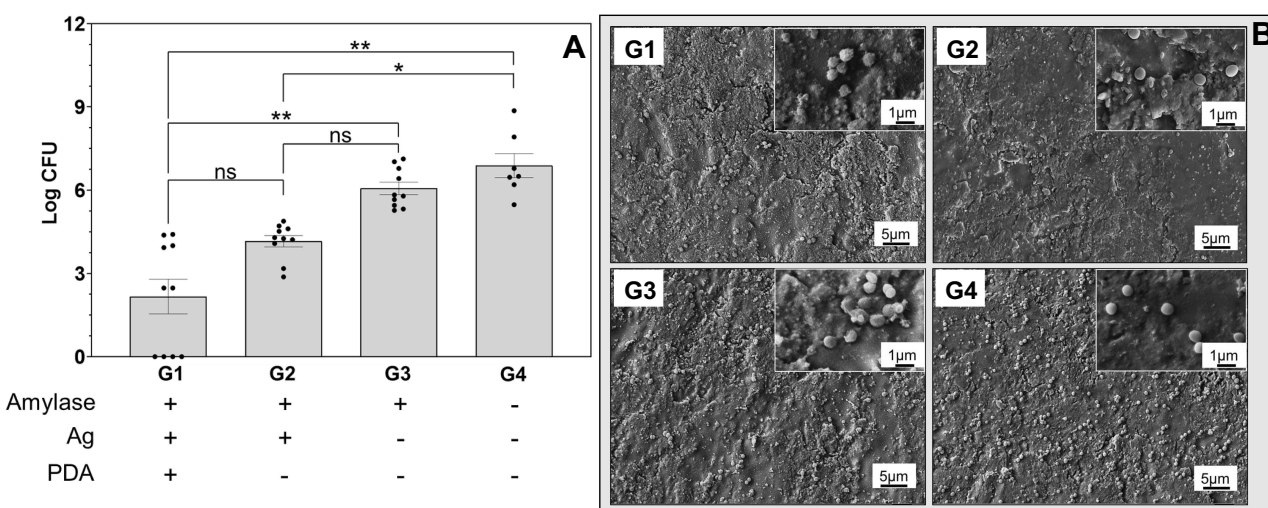


Figure 2 PDA-assisted treatment had higher bacteria killing. **(A)** Colony-forming units (CFU, log scale) recovered from the substrates after the treatment (data = mean \pm standard error of the mean, $n=5$, $*p < 0.05$, $**p < 0.001$). **(B)** Representative SEM images of the sample surface after the treatments.

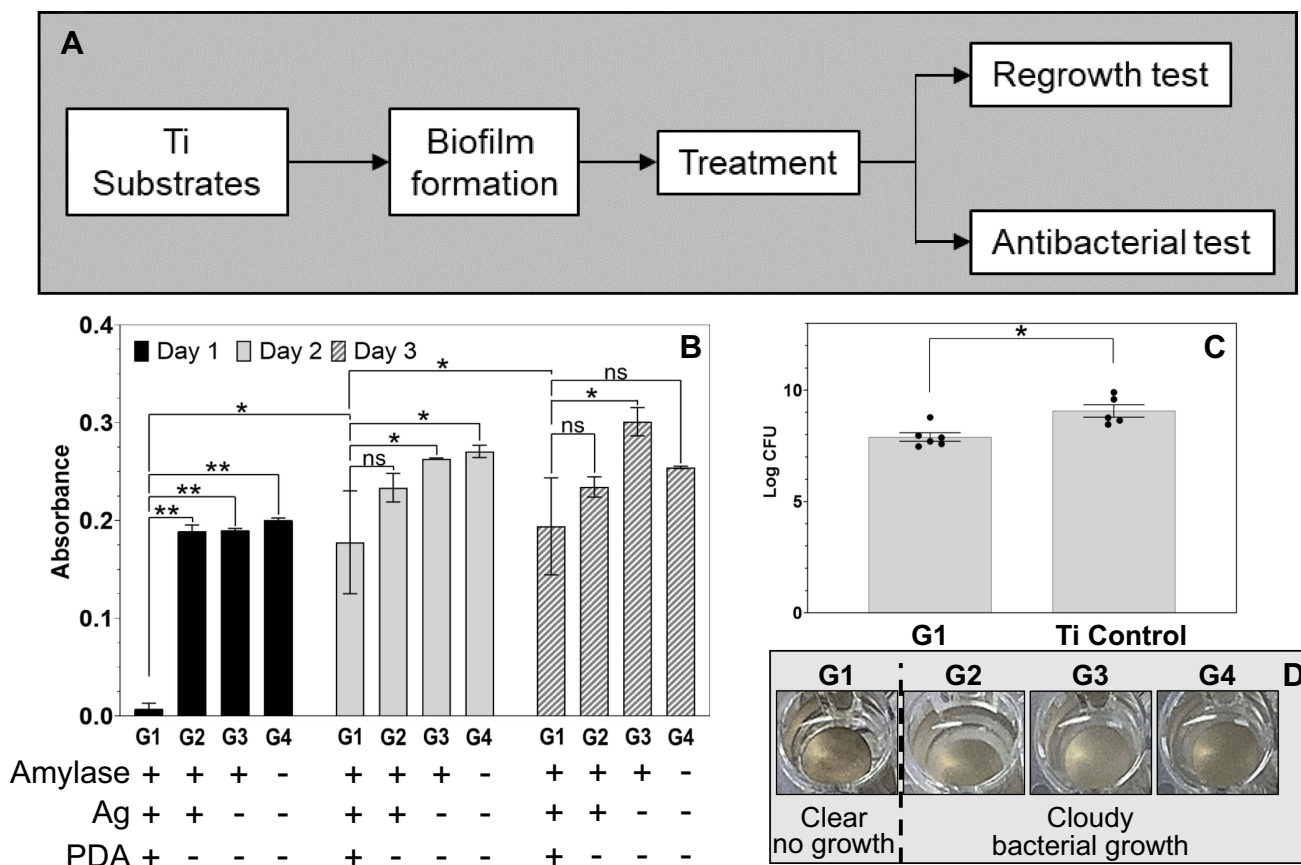


Figure 3 PDA-assisted treatment rendered the surface antimicrobial. **(A):** Procedure of the tests. **(B):** Regrowth of bacteria from treated samples monitored by OD measurement (data = mean \pm standard error of the mean, $n=2$). **(C):** Significant lower log CFU on G1 compared to Ti control. (data = mean \pm standard error of the mean, $n=3$). * $p<0.05$, ** $p<0.001$. **(D):** Photographs showing the turbidity of the broth indicating bacterial growth except for the G1 group.

Ag appeared as submicron-/nanoparticles on the surface as shown in Figure 4B. The spectra from PDA-assisted treatment also showed that more Ag was found on the bacteria with seemingly damaged membrane (Figure 4B1). Higher levels of C and O were also found on bacteria as expected (Figure 4B2). Combining SE imaging and BSE imaging revealed that the majority of immobilized Ag was in the form of nanoparticles of less than 50 nm in diameters (Figure 4C). In contrast, there was no detectable Ag found immobilized on the surface of samples in the Am-Ag treatment group, neither on the bacteria surface nor on the surrounding area (Figure 4B3–4). Thus, the results indicated that PDA facilitated the formation and immobilization of Ag particles from silver nitrate solution onto the substrates.

Discussion

In this study, we investigated our new biomaterial approach in eradicating established biofilms. This study is in the context of implant retention surgery for acute periprosthetic joint infection. For such therapy, it is of critical importance that bacteria

and their biofilms are effectively removed and that the prosthesis surface resistant to bacterial recolonization after the surgery in order to achieve more consistent successful outcomes.^{50,51}

It has been recognized that preventing bacterial recolonization of the implant surface after in situ biofilm treatment is key to reduce reinfection rates.^{50–52} To our best knowledge, there has been no report of a method that eradicates established biofilm on implants in situ and at the same time coats the implant in situ with antimicrobial agents to prevent reinfection.

In this study, we employed the polymerization and self-immobilization chemistry of dopamine and couple this reaction with the biofilm lysis actions of a model enzyme (α -amylase) and bactericidal actions of silver nitrate. We showed that PDA-assisted treatment increased the removal efficacy of the model biofilm and increased the efficacy of killing bacteria compared to treatments without PDA.

Importantly, we found that the PDA-assisted treatment also induced Ag immobilization in the forms of submicron-/

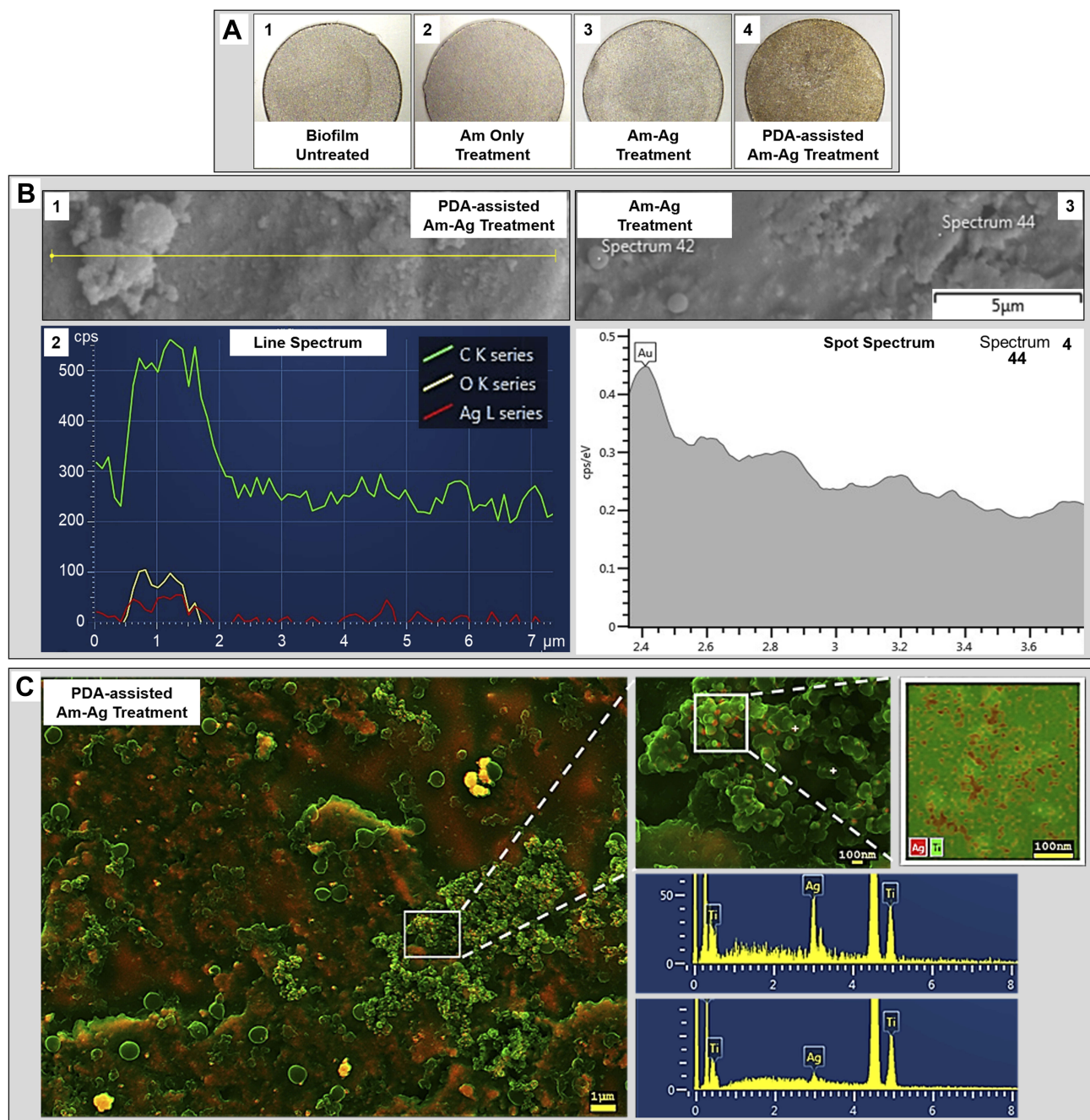


Figure 4 PDA-assisted treatment immobilized the silver particles onto the substrate's surface. **(A)**: Gross appearance of samples showing clear visual color changes in the PDA-assisted treatment group. **(B)**: EDX analysis of Am-Ag treatment and PDA-assisted Am-Ag treatment. B1-2: Line analysis on the PDA-assisted treatment sample shows a clear association of Ag (red Ag spectrum line) with bacteria (C and O lines). B3-4: Point analysis on Am-Ag treatment showing no detectable Ag peaks. **(C)**: A representative pseudo-color merged secondary electron (SE, assigned green color) and backscatter electron (BSE, assigned red color) image showing the distribution of immobilized Ag particles (appeared in bright yellow) in PDA-assisted treatment group. EDX spot analysis and mapping, confirming the presence of Ag and its distribution.

nano-particles on the sample surface. The reduction of Ag ions into Ag particles and their immobilization was attributed to electron transfer with quinone structures' forming from catechol groups at ortho positions.⁵³⁻⁵⁶ This method has been reported in a number of studies using PDA as a priming layer for coating metal nanoparticles on surfaces in a process

similar to our current study. For example, hydroxyapatite on stainless steel substrates was first coated with PDA that then facilitated the formation and immobilization of Ag nanoparticles from ionic Ag solution.^{53,56} Recently, the same method was used to immobilize Ag and Au nanoparticles on PET and silicon wafer surface.⁵⁷

Our bacterial biofilm treatment mechanism was based on the enzyme's disruption of the biofilm extracellular matrix and the Ag's bactericidal activity. First, we established bacterial biofilms, and then PDA was applied as a priming layer prior to the application of the enzyme. Subsequently, the priming-applying process was repeated for the application of Ag. The rationale of the PDA treatment including the first PDA was that the adhered PDA would help immobilize the agents (including enzyme, Ag) from the solution onto the biofilm/bacterial layer, thus enhancing the agent-biofilm interactions. However, in this process, it was possible that the PDA crossed through the biofilm/bacterial layer at some places and hence attached to the Ti surface. It was also recognized that the PDA treatment could be combined with enzyme and antimicrobial at the same time, hence eliminating multiple PDA applications. We are currently optimizing this combination in our laboratories.

Our current work is a proof-of-concept study and thus has several limitations that could be further improved. The biofilms in our study were only a few days old thus were not replicating exactly the biofilms expected in joint space. Our biofilms, however, are still sufficient for us to demonstrate as a proof of concept the effects of the treatment. Further studies would need to replicate better the biofilms, for example, by culturing in dynamic conditions for a longer period of time. In addition, more in-depth experiments with different types of bacteria, enzymes, and antimicrobials of different concentrations should be tested. Investigation of the sizes and density of the immobilized silver particles in the context of surface antimicrobial activity and tissue reintegration should also be conducted in future in vitro and in vivo studies.

Conclusion

In summary, we showed a proof of concept that using the polymerization and self-immobilizing chemistry of dopamine at a mild, aqueous condition, we could enhance biofilm removal and bacterial killing efficacy of the biofilm-lysis enzyme, α -amylase and antimicrobial silver on a model mature *S. aureus* biofilm. Importantly, the same process also deposited antimicrobial silver in situ onto the surface as an antimicrobial coating. These findings suggest that this immobilization-enhanced treatment concept and, in particular, polydopamine-assisted treatment strategy could be promising in the development of advanced in situ treatments for infected devices in implant-retention surgeries.

Acknowledgments

PAT would like to acknowledge his Advance Queensland Research Fellowship (AQR04816-17RD2) and QUT's Vice Chancellor's Research Fellowship. We would like to acknowledge QUT's Central Analytical Research Facility for instrument access.

Disclosure

The authors report no conflicts of interest in this work.

References

- Jämsen E, Stogiannidis I, Malmivaara A, Pajamäki J, Puolakka T, Kontinen YT. Outcome of prosthesis exchange for infected knee arthroplasty: the effect of treatment approach. *Acta Orthop.* 2009;80(1):67–77. doi:10.1080/17453670902805064
- Konrads C, Franz A, Hoberg M, Rudert M. Similar outcomes of two-stage revisions for infection and one-stage revisions for aseptic revisions of knee endoprostheses. *J Knee Surg.* 2018;36:48–50.
- Kunutsor SK, Beswick AD, Whitehouse MR, Wylde V, Blom AW. Debridement, antibiotics and implant retention for periprosthetic joint infections: A systematic review and meta-analysis of treatment outcomes. *J Infect.* 2018;77(6):479–488. doi:10.1016/j.jinf.2018.08.017
- Masters JPM, Smith NA, Foguet P, Reed M, Parsons H, Sprowson AP. A systematic review of the evidence for single stage and two stage revision of infected knee replacement. *BMC Musculoskelet Disord.* 2013;14:222. doi:10.1186/1471-2474-14-222
- Lu J, Han J, Zhang C, Yang Y, Yao Z. Infection after total knee arthroplasty and its gold standard surgical treatment: spacers used in two-stage revision arthroplasty. *Intractable Rare Dis Res.* 2017;6(4):256–261. doi:10.5582/irdr.2017.01049
- Kuiper JW, Willink RT, Moojen DJF, van den Bekerom MP, Colen S. Treatment of acute periprosthetic infections with prosthesis retention: review of current concepts. *World J Orthop.* 2014;5(5):667–676. doi:10.5312/wjo.v5.i5.667
- Qasim SN, Swann A, Ashford R. The DAIR (debridement, antibiotics and implant retention) procedure for infected total knee replacement – a literature review. *Sicot-J.* 2017;3:2. doi:10.1051/sicotj/2016038
- Osmon DR, Berbari EF, Berendt AR, et al. Executive summary: diagnosis and management of prosthetic joint infection: clinical practice guidelines by the infectious diseases society of America. *Clin Infect Dis.* 2012;56(1):1–10. doi:10.1093/cid/cis966
- Ottesen CS, Troelsen A, Sandholdt H, Jacobsen S, Husted H, Gromov K. Acceptable success rate in patients with periprosthetic knee joint infection treated with debridement, antibiotics, and implant retention. *J Arthroplasty.* 2019;34(2):365–368. doi:10.1016/j.arth.2018.09.088
- Zaruta DA, Qiu B, Liu AY, Ricciardi BF. Indications and guidelines for debridement and implant retention for periprosthetic hip and knee infection. *Curr Rev Musculoskelet Med.* 2018;11(3):347–356. doi:10.1007/s12178-018-9497-9
- Hall-Stoodley L, Stoodley P. Evolving concepts in biofilm infections. *Cell Microbiol.* 2009;11(7):1034–1043. doi:10.1111/cmi.2009.11.issue-7
- Lynch AS, Robertson GT. Bacterial and fungal biofilm infections. *Annu Rev Med.* 2008;59(1):415–428. doi:10.1146/annurev.med.59.110106.132000
- Mirza YH, Tansey R, Sukeik M, Shaath M, Haddad FS. Biofilm and the role of antibiotics in the treatment of periprosthetic hip and knee joint infections. *Open Orthop J.* 2016;10(1):636–645. doi:10.2174/1874325001610010636
- Silva M, Tharani R, Schmalzried TP. Results of direct exchange or debridement of the infected total knee arthroplasty. *Clin Orthop Relat Res.* 2002;404:125–131. doi:10.1097/00003086-200211000-00022

15. Leta TH, Lygre SHL, Schrama JC, et al. Outcome of revision surgery for infection after total knee arthroplasty. *JBJS Rev.* 2019;7(6):1. doi:10.2106/JBJS.RVW.18.00084
16. Sherrell JC, Fehring TK, Odum S, et al. The Chitranjan Ranawat Award: fate of two-stage reimplantation after failed irrigation and débridement for periprosthetic knee infection. *Clin Orthop Relat Res.* 2011;469(1):18–25. doi:10.1007/s11999-010-1434-1
17. Urish KL, Bullock AG, Kreger AM, et al. A multicenter study of irrigation and debridement in total knee arthroplasty periprosthetic joint infection: treatment failure is high. *J Arthroplasty.* 2018;33(4):1154–1159. doi:10.1016/j.arth.2017.11.029
18. Gnanadhas DP, Elango M, Janardhanraj S, et al. Successful treatment of biofilm infections using shock waves combined with antibiotic therapy. *Sci Rep.* 2015;5:1–13. doi:10.1038/srep17440
19. Qi X, Zhao Y, Zhang J, et al. Increased effects of extracorporeal shock waves combined with gentamicin against staphylococcus aureus biofilms in vitro and in vivo. *Ultrasound Med Biol.* 2016;42(9):2245–2252. doi:10.1016/j.ultrasmedbio.2016.04.018
20. Barra F, Roscetto E, Soriano AA, et al. Photodynamic and antibiotic therapy in combination to fight biofilms and resistant surface bacterial infections. *Int J Mol Sci.* 2015;16(9):20417–20430. doi:10.3390/ijms160920417
21. Estellés A, Woischnig A-K, Liu K, et al. A high-affinity native human antibody disrupts biofilm from Staphylococcus aureus bacteria and potentiates antibiotic efficacy in a mouse implant infection model. *Antimicrob Agents Chemother.* 2016;60(4):2292–2301. doi:10.1128/AAC.02588-15
22. García I, Ballesta S, Gilaberte Y, Rezusta A, Pascual Á. Antimicrobial photodynamic activity of hypericin against methicillin-susceptible and resistant Staphylococcus aureus biofilms. *Future Microbiol.* 2015;10(3):347–356. doi:10.2217/fmb.14.114
23. Mai B, Wang X, Liu Q, et al. The antibacterial effect of sinoporphyrin sodium photodynamic therapy on Staphylococcus aureus planktonic and biofilm cultures. *Lasers Surg Med.* 2016;48(4):400–408. doi:10.1002/lsm.22468
24. Pérez-Laguna V, Pérez-Artiaga L, Lampaya-Pérez V, et al. Bactericidal effect of photodynamic therapy, alone or in combination with mupirocin or linezolid, on Staphylococcus aureus. *Front Microbiol.* 2017;8:1–9. doi:10.3389/fmicb.2017.01002
25. Rosa LP, Da Silva FC, Nader SA, Meira GA, Viana MS. Antimicrobial photodynamic inactivation of Staphylococcus aureus biofilms in bone specimens using methylene blue, toluidine blue ortho and malachite green: an in vitro study. *Arch Oral Biol.* 2015;60(5):675–680. doi:10.1016/j.archoralbio.2015.02.010
26. Xiong YQ, Estellés A, Li L, et al. A human biofilm-disrupting monoclonal antibody potentiates antibiotic efficacy in rodent models of both Staphylococcus aureus and Acinetobacter baumannii infections. *Antimicrob Agents Chemother.* 2017;61(10):e00904–e00917. doi:10.1128/AAC.00904-17
27. Bradford C. The use of commercially available alpha-amylase compounds to inhibit and remove Staphylococcus aureus biofilms. *Open Microbiol J.* 2011;5(1):21–31. doi:10.2174/1874285801105010021
28. Ceotto-Vigoder H, Marques SLS, Santos INS, et al. Nisin and lysostaphin activity against preformed biofilm of Staphylococcus aureus involved in bovine mastitis. *J Appl Microbiol.* 2016;121(1):101–114. doi:10.1111/jam.2016.121.issue-1
29. Fleming D, Chahin L, Rumbaugh K. Glycoside hydrolases degrade polymicrobial bacterial biofilms in wounds. *Antimicrob Agents Chemother.* 2017;61(2):e01998–16.
30. Kaplan JB, Lovetri K, Cardona ST, et al. Recombinant human DNase i decreases biofilm and increases antimicrobial susceptibility in staphylococci. *J Antibiot.* 2012;65(2):73–77. doi:10.1038/ja.2011.113
31. Kokai-Kun JF, Chanturiya T, Mond JJ. Lysostaphin eradicates established Staphylococcus aureus biofilms in jugular vein catheterized mice. *J Antimicrob Chemother.* 2009;64(1):94–100. doi:10.1093/jac/dkp145
32. Meireles A, Borges A, Giaouris E, Simões M. The current knowledge on the application of anti-biofilm enzymes in the food industry. *Food Res Int.* 2016;86:140–146. doi:10.1016/j.foodres.2016.06.006
33. Chernousova S, Epple M. Silver as antibacterial agent: ion, nanoparticle, and metal. *Angew Chem Int Ed.* 2013;52(6):1636–1653. doi:10.1002/anie.v52.6
34. Marambio-Jones C, Hoek EMV. A review of the antibacterial effects of silver nanomaterials and potential implications for human health and the environment. *J Nanopart Res.* 2010;12(5):1531–1551. doi:10.1007/s11051-010-9900-y
35. Sawai J. Quantitative evaluation of antibacterial activities of metallic oxide powders (ZnO, MgO and CaO) by conductimetric assay. *J Microbiol Methods.* 2003;54(2):177–182. doi:10.1016/S0167-7012(03)00037-X
36. VV, Anthony SP. Antimicrobial studies of metal and metal oxide nanoparticles. *Surface Chemistry of Nanobiomaterials.* 2016:265–300. doi:10.1016/b978-0-323-42861-3.00009-1
37. Lok C-N, Ho C-M, Chen R, et al. Silver nanoparticles: partial oxidation and antibacterial activities. *JBIC J Biol Inorg Chem.* 2007;12(4):527–534. doi:10.1007/s00775-007-0208-z
38. Liao Y, Wang Y, Feng X, Wang W, Xu F, Zhang L. Antibacterial surfaces through dopamine functionalization and silver nanoparticle immobilization. *Mater Chem Phys.* 2010;121(3):534–540. doi:10.1016/j.matchemphys.2010.02.019
39. Ryu JH, Messersmith PB, Lee H. Polydopamine surface chemistry: a decade of discovery. *ACS Appl Mater Interfaces.* 2018;10(9):7523–7540. doi:10.1021/acsami.7b19865
40. Saidin S, Chevallier P, Abdul Kadir MR, Hermawan H, Mantovani D. Polydopamine as an intermediate layer for silver and hydroxyapatite immobilisation on metallic biomaterials surface. *Mater Sci Eng C.* 2013;33(8):4715–4724. doi:10.1016/j.msec.2013.07.026
41. Sileika TS, Kim HD, Maniak P, Messersmith PB. Antibacterial performance of polydopamine-modified polymer surfaces containing passive and active components. *ACS Appl Mater Interfaces.* 2011;3(12):4602–4610. doi:10.1021/am200978h
42. Lee H, Dellatore SM, Miller WM, Messersmith PB. Mussel-inspired surface chemistry for multifunctional coatings. *Science.* 2007;318(5849):426–430. doi:10.1126/science.1147241
43. Cong Y, Xia T, Zou M, et al. Mussel-inspired polydopamine coating as a versatile platform for synthesizing polystyrene/Ag nanocomposite particles with enhanced antibacterial activities. *J Mater Chem B.* 2014;2(22):3450–3461. doi:10.1039/C4TB00460D
44. Liu X, Cao J, Li H, et al. Mussel-inspired polydopamine: a biocompatible and ultrastable coating for nanoparticles in vivo. *ACS Nano.* 2013;7(10):9384–9395. doi:10.1021/nn404117j
45. Qu R, Zhang W, Liu N, et al. Antioil Ag3PO4 nanoparticle/polydopamine/Al2O3 sandwich structure for complex wastewater treatment: dynamic catalysis under natural light. *ACS Sustain Chem Eng.* 2018;6(6):8019–8028. doi:10.1021/acsuschemeng.8b01469
46. Khan S, Tøndervik A, Sletta H, et al. Overcoming drug resistance with alginate oligosaccharides able to potentiate the action of selected antibiotics. *Antimicrob Agents Chemother.* 2012;56(10):5134–5141. doi:10.1128/AAC.00525-12
47. Hajipour MJ, Fromm KM, Akbar Ashkarran A, et al. Antibacterial properties of nanoparticles. *Trends Biotechnol.* 2012;30(10):499–511. doi:10.1016/j.tibtech.2012.06.004
48. Le Ouay B, Stellacci F. Antibacterial activity of silver nanoparticles: a surface science insight. *Nano Today.* 2015;10(3):339–354. doi:10.1016/j.nantod.2015.04.002
49. Tang S, Zheng J. Antibacterial activity of silver nanoparticles: structural effects. *Adv Healthc Mater.* 2018;7(13):1–10. doi:10.1002/adhm.v7.13
50. Argenson JN, Arndt M, Babis G, et al. Hip and knee section, treatment, debridement and retention of implant: proceedings of international consensus on orthopedic infections. *J Arthroplasty.* 2019;34(2, Supplement):S399–S419. doi:10.1016/j.arth.2018.09.025

51. Vilchez F, Martínez-Pastor JC, García-Ramiro S, et al. Efficacy of debridement in hematogenous and early post-surgical prosthetic joint infections. *Int J Artif Organs*. 2011;34(9):863–869. doi:10.5301/ijao.5000029
52. Dietz MJ, Bostian PA, Ernest EP, et al. Rate of surface contamination in the operating suite during revision total joint arthroplasty. *Arthroplast Today*. 2018;5(1):96–99. doi:10.1016/j.artd.2018.09.007
53. Jahed FS, Hamidi S, Nemati M. Dopamine-capped silver nanoparticles as a colorimetric probe for on-site detection of cyclosporine. *ChemistrySelect*. 2018;3(47):13323–13328. doi:10.1002/slct.v3.47
54. Waite JH. Adhesion a la moule. *Integr Comp Biol*. 2002;42(6):1172–1180. doi:10.1093/icb/42.6.1172
55. Waite JH, Tanzer ML. Polyphenolic substance of mytilus edulis: novel adhesive containing L-dopa and hydroxyproline. *Science*. 1981;212(4498):1038–1040. doi:10.1126/science.212.4498.1038
56. Yoosaf K, Ipe BI, Suresh CH, Thomas KG. In situ synthesis of metal nanoparticles and selective naked-eye detection of lead ions from aqueous media. *J Phys Chem C*. 2007;111(34):12839–12847. doi:10.1021/jp073923q
57. Chang T-L, Yu X, Liang JF. Polydopamine-enabled surface coating with nano-metals. *Surf Coat Technol*. 2018;337:389–395. doi:10.1016/j.surfcoat.2018.01.009

International Journal of Nanomedicine

Dovepress

Publish your work in this journal

The International Journal of Nanomedicine is an international, peer-reviewed journal focusing on the application of nanotechnology in diagnostics, therapeutics, and drug delivery systems throughout the biomedical field. This journal is indexed on PubMed Central, MedLine, CAS, SciSearch®, Current Contents®/Clinical Medicine,

Journal Citation Reports/Science Edition, EMBase, Scopus and the Elsevier Bibliographic databases. The manuscript management system is completely online and includes a very quick and fair peer-review system, which is all easy to use. Visit <http://www.dovepress.com/testimonials.php> to read real quotes from published authors.

Submit your manuscript here: <https://www.dovepress.com/international-journal-of-nanomedicine-journal>